

Real-time implementation of digital relay models using MATLAB/SIMULINK and RTDS

Christos A. Apostolopoulos^{*,†} and George N. Korres

School of Electrical and Computer Engineering, National Technical University of Athens, Greece

SUMMARY

In this paper, an integrated environment for real-time simulation, analysis and validation of digital relay models, based on MATLAB/SIMULINK and RTDS, is presented. A detailed analysis and discussion for this environment is given and example cases are used to illustrate its implementation. Copyright © 2008 John Wiley & Sons, Ltd.

KEY WORDS: digital relay model; MATLAB/SIMULINK; RTDS

1. INTRODUCTION

Software models for protective relays offer an economic and feasible alternative to studying the performance of protective relays. Relay models have been long used in a variety of tasks, such as designing new relaying algorithms, optimizing relay settings and training personnel [1].

In order to be practical, software relay models must reproduce the actual operation of the physical relays. This has been somewhat difficult for electromechanical relays, due to lack of design data. In the case of digital relays, which are the prevailing practice in today's power systems, this has become simpler. Most of the digital relays are accompanied by technical manuals that describe adequately their algorithms and design characteristics. Based on this information, fairly "accurate" digital relay models can be developed, by using a high level language such as FORTRAN, C, C++[2], or commercial software packages like MATLAB, SIMULINK [3].

In most of the existing applications, digital relay models are used in conjunction with electromagnetic transient programs (EMTP) for off-line open or closed-loop simulation studies [4,5]. Although these applications are useful for relay performance evaluation, it would be desirable to have a real-time implementation of digital relay models. A real-time implementation would enhance the realism of the models and would provide access to hardware and software issues currently not available in off-line simulation studies.

Real-time applications make necessary the use of specific devices, like microprocessors and DSPs. These devices require reprogramming of the digital relay model with special machine code, which is a difficult and time consuming task. Also, in order to be practical, the real-time platform needs to be cost effective and easy to set up.

In this paper, a low-cost platform is proposed based on MATLAB/SIMULINK, which is used not only as a simulation tool for developing digital relay models, but principally for their real-time execution. By using a general purpose data acquisition board (DAB), the developed digital relay model can act as a physical relay and be integrated with a real-time digital simulator (RTDS) forming thus a hardware-in-the-loop simulation environment [6].

*Correspondence to: Christos A. Apostolopoulos, School of Electrical and Computer Engineering, National Technical University of Athens, Greece.

†E-mail: apostolo@power.ece.ntua.gr

RTDSs have been traditionally used for closed-loop testing of physical devices, such as controllers and protective relays. If in the place of the physical device a real-time digital relay model were used, an efficient approach would be established for rapid prototyping of new relay designs and studying existing relaying algorithms.

In the following sections, the proposed environment for real-time implementation of digital relay models, combining MATLAB, SIMULINK, and RTDS is presented. A multifunctional digital relay model, developed in SIMULINK, is also described in detail. Finally, for demonstration purposes, example cases are given.

2. THE INTEGRATED SIMULATION ENVIRONMENT

The proposed simulation environment is based on the RTDS, and the real-time resources of MATLAB/SIMULINK. RTDS is used for modeling the power system network; whereas MATLAB/SIMULINK is used for developing and implementing the digital relay models.

2.1. Real time digital simulator (RTDS)

The RTDS is a fully digital power system simulator capable of continuous real time operation [7]. It performs electromagnetic transient simulations with a typical time step of 50 μ second utilizing a combination of custom software and hardware.

RTDS hardware comprises different types of processor cards, signal channels, and communication modules. An Ethernet connection is used to transfer data between the hardware and the interfaced computer. External devices can be connected to the RTDS *via* digital and analog I/O channels.

The software, by which the user enters, saves, and compiles the graphically driven system for simulation operation in the RTDS, is called RSCAD. Predefined control-blocks and scripts can be used to control the simulations. During the simulation the user can monitor specified system quantities or dynamically interact with the simulation as it runs.

The connection of the RTDS with external devices allows performing closed loop testing of physical equipment such as protective relays and control systems. Closed loop testing is performed by receiving output signals from the simulation and using them as inputs to the device under test. The output of the device is then fed back into the simulation. This type of device testing resembles its actual performance [8].

2.2. MATLAB/SIMULINK

MATLAB is a world-wide recognized software package, for modeling, simulating, and analyzing dynamic systems. MATLAB comes along with SIMULINK, which is MATLAB's time domain solver. SIMULINK supports linear and nonlinear systems modeled in continuous time, sampled time and a combination of both. Different parts of a system can be also sampled at different rates. SIMULINK has a powerful graphical user interface, which allows rapid development with great visualization capabilities.

MATLAB/SIMULINK provides a well-known tool for modeling digital protective relays. SIMULINK offers a wide selection of libraries that allow detailed simulation of the hardware and software parts of digital relays. Aspects of digital relaying, such as signal conditioning, analog-to-digital conversion, digital filtering, phasor estimation, protection algorithms, and relay trip logic, can be modeled using general purpose blocks, special blocks from the signal processing blockset and user-defined blocks written in S-functions [9].

A digital relay model developed in SIMULINK can be used in open loop simulation studies with fault waveforms obtained from fault-recorded data, captured by DFRs or from software simulation. It can also take part in closed-loop simulation studies if it is used along with SimPowerSystem Blockset. SimPowerSystem Blockset is a new extension of MATLAB, which provides computations similar to EMTP, permitting modeling of both the power system and its control in the same environment.

Finally, it can be executed in real-time using real-time workshop (RTW) [10] and SIMULINK in external mode. RTW is a SIMULINK library that produces an executable file. Real-time windows target (RTWT) [11] is a library that executes in real-time the file compiled by RTW. It also allows the SIMULINK model to be connected to various commercial data-acquisition cards (DAC), thus interfacing MATLAB/SIMULINK to the computer's external environment. Managing the process in real time is achieved on the same computer entirely by the use of MATLAB/SIMULINK.

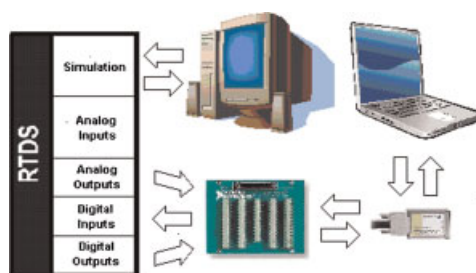


Figure 1. Schematic diagram of the proposed environment.

2.3. Integration of MATLAB/SIMULINK and RTDS

A schematic diagram of the proposed integrated simulation environment is shown in Figure 1. MATLAB/SIMULINK is installed on a notebook PC together with its real time packages. A DAC, responsible for receiving and sending signals to the RTDS, is also included. The operation characteristics of the data acquisition card are shown in Table I.

The RSCAD software, which controls the real-time simulation in the RTDS, is installed on a separate personal computer host. A power system model can be created using RSCAD. This model includes the representation of all the power system components, such as sources, transmission lines, instrument transformers, circuit breakers and switchable symmetric or asymmetric faults. It is compiled and downloaded to the RTDS rack, where it runs continuously in real-time, until halted by the user.

When compiling the real-time power system model, certain system variables can be sent to the digital and analog output ports of the RTDS rack. In the case of protective relays, the variables of interest are the instantaneous voltages and currents in the secondary circuits of the VTs and CTs located at the relay position. These voltage and current signals, as computed by the simulation, are sent to the six channels of two high-precision analog output cards of the RTDS rack.

The low-level analog signals generated from the RTDS are scaled properly and sent to the analog input ports of the DAC. The signals are read from the DAC and passed into the digital relay model, which is executed in real-time at the MATLAB/SIMULINK environment as a stand-alone application. The relay model processes these signals and initiate actions according to the protection algorithms and relay settings applied. The relay trip and reclosing signals can be assigned to different digital output ports of the DAC and can be sent to individual bits of a TTL-level digital input port of the RTDS rack. These bits control the breaker statuses of the power system model in the RTDS and are internally pulled up to +5 volts, in order to provide voltage to wet the digital output ports of the DAC.

3. THE DIGITAL RELAY MODEL

A multi-functional digital relay model has been developed in the MATLAB/SIMULINK environment, using a modular approach (each part of the relay hardware and software is implemented as a separate function). Each function has been created using special

Table I. Characteristics of the data acquisition card.

Family	NI DAQCard-6036E
Bus	PCMCIA
Analog inputs	16 SE/8 DIF
Input resolution	16 bits
Max sampling rate	200 kS/second
Input range	± 0.05 – ± 10 V
Digital I/O	8

blocks of SIMULINK and signal processing libraries. The most complicated functions have been developed as masked subsystems, with S-functions performing the required operations.

In the following, the main functions included in the digital relay model are presented.

3.1. Real-time data acquisition

An analog input block from the RTWT Library is used to define the parameters of the DAC. The DAC performs the tasks of sampling and digitizing the low-level analog voltage signals received from the RTDS analog output channels. The analog input block allows to set the sampling interval period in the DAQ card, to define the AI channels in the DAQ card passed into the real-time simulation and to select the range of the input signals' representation.

Usually, digital relays filter their analog input signals with a low-pass analog filter, in order to prevent anti-aliasing. Because the DAB used does not support a built-in signal conditioning unit, this function is not included in the digital relay model. A high-pass digital filter is used to smooth and remove noise from the sampled data.

3.2. Phasor estimation and frequency tracking

A full-cycle discrete fourier transform (DFT) is used to estimate the fundamental frequency phasors of the received discrete voltage and current signals. The phasor estimates of these signals at time sample r are given by

$$\begin{aligned} \bar{X}^{(r)} &= \frac{\sqrt{2}}{N} \sum_{k=r-N}^{r-1} x(k\Delta T) e^{-\frac{j2\pi k}{N}} \\ &= \frac{\sqrt{2}}{N} \sum_{k=r-N}^{r-1} x(k\Delta T) \cos\left(\frac{2\pi k}{N}\right) - j \frac{\sqrt{2}}{N} \sum_{k=r-N}^{r-1} x(k\Delta T) \sin\left(\frac{2\pi k}{N}\right) \\ &= X_R^{(r)} + jX_I^{(r)} \end{aligned} \quad (1)$$

The rms magnitude and phase angle of the estimated phasors are calculated by

$$|\bar{X}^{(r)}| = \sqrt{X_R^{(r)2} + X_I^{(r)2}} \quad (2)$$

$$\theta^{(r)} = \angle \bar{X}^{(r)} = \arctan\left(\frac{X_I^{(r)}}{X_R^{(r)}}\right) \quad (3)$$

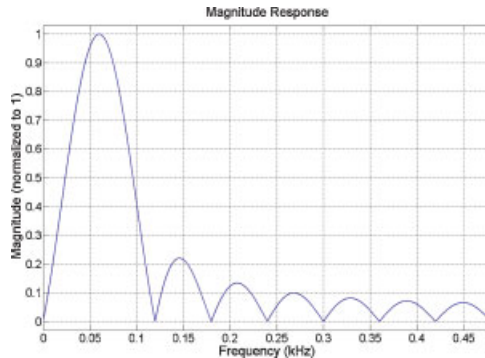


Figure 2. Frequency response of 16-point DFT with sampling rate of 960 Hz.

Due to the fact that the sampling frequency used is 960 Hz, the required number of samples per cycle, for a full-cycle DFT, is $N = 16$. The frequency response up to the Nyquist frequency of the used 16-point DFT, is shown in Figure 2.

As it can be seen from Figure 2, the 16-point DFT filter cancels all harmonics up to the Nyquist frequency, except from the fundamental. The estimate of the fundamental frequency phasor is correct, as long as the signal being sampled is exactly at 60 Hz. However this is not always the case in power system networks. Frequency excursions exist and can take significant values, in case of a power swing or near to generation plants.

The DFT magnitude will not change significantly if the system frequency is not far from the nominal, as it can be seen in Figure 2. For large frequency deviations, the DFT will be affected considerably and this will cause problems in frequency dependent variables of the digital relay, such as the calculated impedances. In order to allow for frequency excursions, a frequency-tracking algorithm which compensates for the phasor estimates has been developed [12–15].

The first step of the frequency-tracking algorithm is to provide an estimate of the prevailing power system frequency. This is done by calculating at each time step the phase deviation phasors of each phase voltage $\bar{D}_a, \bar{D}_b, \bar{D}_c$ [12]:

$$\begin{aligned}\bar{D}_a^{(r)} &= \bar{U}_a^{(r)} \bar{U}_a^{(r-1)*} \\ &= \left(U_{aR}^{(r)} U_{aR}^{(r-1)} + U_{aI}^{(r)} U_{aI}^{(r-1)} \right) + j \left(U_{aI}^{(r)} U_{aR}^{(r-1)} - U_{aR}^{(r)} U_{aI}^{(r-1)} \right)\end{aligned}\quad (4)$$

$$\begin{aligned}\bar{D}_b^{(r)} &= \bar{U}_b^{(r)} \bar{U}_b^{(r-1)*} \\ &= \left(U_{bR}^{(r)} U_{bR}^{(r-1)} + U_{bI}^{(r)} U_{bI}^{(r-1)} \right) + j \left(U_{bI}^{(r)} U_{bR}^{(r-1)} - U_{bR}^{(r)} U_{bI}^{(r-1)} \right)\end{aligned}\quad (5)$$

$$\begin{aligned}\bar{D}_c^{(r)} &= \bar{U}_c^{(r)} \bar{U}_c^{(r-1)*} \\ &= \left(U_{cR}^{(r)} U_{cR}^{(r-1)} + U_{cI}^{(r)} U_{cI}^{(r-1)} \right) + j \left(U_{cI}^{(r)} U_{cR}^{(r-1)} - U_{cR}^{(r)} U_{cI}^{(r-1)} \right)\end{aligned}\quad (6)$$

The phase deviation phasors do not rotate to each other and the phase angle of each phase deviation phasor with respect to the real axis is the same for each respective phase. Thus, they can be added directly to produce the frequency deviation phasor \bar{D} :

$$\bar{D} = \bar{D}_a + \bar{D}_b + \bar{D}_c \quad (7)$$

The frequency deviation phasor \bar{D} is provided to a first-order digital low-pass filter with a time constant t_c equal to 0.05 second. This filter removes noise from the frequency deviation phasor and has the following iterative form:

$$y_k = (1 - a)y_{k-1} + ax_k \quad (8)$$

where $(1 - a) = \Delta T/t_c + \Delta T$, $a = \Delta T/t_c - \Delta T$, and $t_c = 0.05$.

The actual system frequency is related to the f filtered frequency deviation phasor \bar{D}' according to the following equation [13]:

$$f^{(r)} = \left(\frac{1}{2\pi} \tan^{-1} \left(\frac{\text{Im}(\bar{D}'^{(r)})}{\text{Re}(\bar{D}'^{(r)})} \right) + 1 \right) f_0 \quad (9)$$

The knowledge of the actual frequency at each time step allows to compensate for the phasor estimates of voltages and currents as calculated by Equation (1), assuming a constant frequency equal to the nominal. This can be done using the following approach [14,15]:

A real valued sinusoidal signal with a frequency f can be expressed as

$$x(t) = \text{Re}(\bar{X}e^{j2\pi ft}) = \frac{\bar{X}e^{j2\pi ft} + \bar{X}^* e^{-j2\pi ft}}{2} \quad (10)$$

Substituting Equation (10) into Equation (1), the following is obtained:

$$\begin{aligned}
 \bar{X}_{f_0+\Delta f}^{(r)} &= \frac{2}{N} \sum_{k=r-N}^{r-1} \frac{\bar{X} e^{j2\pi f t} + \bar{X}^* e^{-j2\pi f t}}{2} e^{-j\frac{2\pi k}{N}} \\
 &= \frac{2}{N} \sum_{k=r-N}^{r-1} \frac{\bar{X} e^{j2\pi f k \Delta T} + \bar{X}^* e^{-j2\pi f k \Delta T}}{2} e^{-j\frac{2\pi k}{N}} \\
 &= \frac{2}{N} \sum_{k=r-N}^{r-1} \frac{\bar{X} e^{j2\pi f k \frac{1}{N f_0}} + \bar{X}^* e^{-j2\pi f k \frac{1}{N f_0}}}{2} e^{-j\frac{2\pi k}{N}} \\
 &= \frac{1}{N} \bar{X} \sum_{k=r-N}^{r-1} e^{j\frac{2\pi k}{N} \left(\frac{f}{f_0}-1\right)} + \frac{1}{N} \bar{X}^* \sum_{k=r-N}^{r-1} e^{-j\frac{2\pi k}{N} \left(\frac{f}{f_0}+1\right)} \\
 &= \frac{1}{N} \bar{X} \sum_{k=r-N}^{r-1} e^{j\frac{2\pi k \Delta f}{N f_0}} + \frac{1}{N} \bar{X}^* \sum_{k=r-N}^{r-1} e^{-j\frac{2\pi k}{N} \left(\frac{\Delta f}{f_0}+2\right)} \\
 &= \frac{1}{N} \bar{X} e^{j\frac{2\pi \Delta f}{N f_0} r} \sum_{k=-N}^{-1} e^{j\frac{2\pi k \Delta f}{N f_0}} + \frac{1}{N} \bar{X}^* e^{-j\frac{2\pi \Delta f}{N f_0} r} \sum_{k=-N}^{-1} e^{-j\frac{2\pi k}{N} \left(\frac{\Delta f}{f_0}+2\right)} \\
 &= \frac{1}{N} \bar{X} e^{j\frac{2\pi \Delta f}{N f_0} r} e^{-j2\pi \frac{\Delta f}{f_0} r} \sum_{k=0}^{N-1} e^{j\frac{2\pi k \Delta f}{N f_0}} + \frac{1}{N} \bar{X}^* e^{-j\frac{2\pi \Delta f}{N f_0} r} e^{j2\pi \frac{\Delta f}{f_0} r} \sum_{k=0}^{N-1} e^{-j\frac{2\pi k}{N} \left(\frac{\Delta f}{f_0}+2\right)} \\
 &= \frac{1}{N} \bar{X} e^{j2\pi \frac{\Delta f}{f_0} \left(\frac{r}{N}-1\right)} \sum_{k=0}^{N-1} e^{j\frac{2\pi k \Delta f}{N f_0}} + \frac{1}{N} \bar{X}^* e^{-j2\pi \frac{\Delta f}{f_0} \left(\frac{r}{N}-1\right)} \sum_{k=0}^{N-1} e^{-j\frac{2\pi k}{N} \left(\frac{\Delta f}{f_0}+2\right)}
 \end{aligned} \tag{11}$$

Equation (11) can be simplified using the following identity:

$$\sum_{i=0}^{N-1} (e^{j\theta})^i = \frac{\sin N\theta/2}{\sin \theta/2} e^{j(N-1)\frac{\theta}{2}} \tag{12}$$

By using equation (12) in equation (11), we have:

$$\begin{aligned}
 \bar{X}_{f_0+\Delta f}^{(r)} &= \frac{1}{N} \bar{X} \frac{\sin \pi \Delta f / f}{\sin \pi \Delta f / N f_0} e^{-j\pi \frac{\Delta f}{f_0} \left(1+\frac{1}{N}\right)} e^{j\frac{\Delta f}{f_0} 2\pi r} \\
 &\quad + \frac{1}{N} \bar{X}^* \frac{\sin \pi \Delta f / f_0}{\sin(2\pi/N + \pi \Delta f / N f_0)} e^{j\pi \frac{\Delta f}{f_0} \left(1+\frac{1}{N}\right)} e^{j\frac{2\pi}{N} r} e^{-j\frac{\Delta f}{f_0} 2\pi r}
 \end{aligned} \tag{13}$$

In Equation (13), $\bar{X}_{f_0+\Delta f}^{(r)}$ is the measured phasor \bar{X}_{meas} and \bar{X} is the exact phasor. The measured phasor can be expressed as a function of the exact phasor, with two correction functions designated \bar{P} and \bar{Q} :

$$\bar{X}_{\text{meas}} = \bar{P}\bar{X} + \bar{Q}\bar{X}^* \tag{14}$$

Correction factors \bar{P} and \bar{Q} are functions of the frequency deviation $\Delta f = f - f_0$ and are defined as follows:

$$\bar{P}(\Delta f)^{(r)} = \frac{1}{N} \frac{\sin \pi \Delta f / f_0}{\sin \pi \Delta f / N f_0} e^{-j\pi \frac{\Delta f}{f_0} \left(1+\frac{1}{N}\right)} e^{j\frac{\Delta f}{f_0} 2\pi r} \tag{15}$$

$$\bar{Q}(\Delta f)^{(r)} = \frac{1}{N} \frac{\sin \pi \Delta f / f_0}{\sin(2\pi/N + \pi \Delta f / N f_0)} e^{j\pi \frac{\Delta f}{f_0} \left(1+\frac{1}{N}\right)} e^{j\frac{2\pi}{N} r} e^{-j\frac{\Delta f}{f_0} 2\pi r} \tag{16}$$

The correction factors \bar{P} and \bar{Q} along with \bar{X}_{meas} and \bar{X} can be expressed with their real and imaginary parts: $\bar{P} = P_R + jP_I$, $\bar{Q} = Q_R + jQ_I$, $\bar{X}_{\text{meas}} = X_{\text{meas}_R} + jX_{\text{meas}_I}$, and $\bar{X} = X_R + jX_I$. It is then possible to express the Cartesian components of the

measured phasor in terms of the exact phasor as follows:

$$\begin{bmatrix} X_{\text{meas_R}}^{(r)} \\ X_{\text{meas_I}}^{(r)} \end{bmatrix} = \begin{bmatrix} (P_R(\Delta f)^{(r)} + Q_R(\Delta f)^{(r)}) & (Q_I(\Delta f)^{(r)} - P_I(\Delta f)^{(r)}) \\ (P_I(\Delta f)^{(r)} + Q_I(\Delta f)^{(r)}) & (P_R(\Delta f)^{(r)} - Q_R(\Delta f)^{(r)}) \end{bmatrix} \begin{bmatrix} X_R^{(r)} \\ X_I^{(r)} \end{bmatrix} \quad (17)$$

The exact (or compensated) phasor can be calculated by inverting the 2×2 matrix in Equation (17):

$$\begin{bmatrix} X_R^{(r)} \\ X_I^{(r)} \end{bmatrix} = \begin{bmatrix} (P_R(\Delta f)^{(r)} + Q_R(\Delta f)^{(r)}) & (Q_I(\Delta f)^{(r)} - P_I(\Delta f)^{(r)}) \\ (P_I(\Delta f)^{(r)} + Q_I(\Delta f)^{(r)}) & (P_R(\Delta f)^{(r)} - Q_R(\Delta f)^{(r)}) \end{bmatrix}^{-1} \begin{bmatrix} X_{\text{meas_R}}^{(r)} \\ X_{\text{meas_I}}^{(r)} \end{bmatrix} \quad (18)$$

in Equation (18), $P_R(\Delta f)$, $Q_R(\Delta f)$, $P_I(\Delta f)$, $Q_I(\Delta f)$ are the real and imaginary parts of the correction factors \bar{P} and \bar{Q} given at sample time r by the following equations:

$$P_R(\Delta f)^{(r)} = \frac{\sin(\Delta f/f_0\pi)}{N \sin(\Delta f/Nf_0\pi)} \cos\left(\frac{\Delta f}{f_0}\pi\left(\frac{2}{N}r - 1 - \frac{1}{N}\right)\right) \quad (19)$$

$$P_I(\Delta f)^{(r)} = \frac{\sin(\Delta f/f_0\pi)}{N \sin(\Delta f/Nf_0\pi)} \sin\left(\frac{\Delta f}{f_0}\pi\left(\frac{2}{N}r - 1 - \frac{1}{N}\right)\right) \quad (20)$$

$$Q_R(\Delta f)^{(r)} = \frac{\sin(\Delta f/f_0\pi)}{N \sin(\Delta f/Nf_0\pi + 2\pi/N)} \cos\left(\frac{\Delta f}{f_0}\pi\left(1 + \frac{1}{N} - \frac{2}{N}r\right) + \frac{2\pi}{N}\right) \quad (21)$$

$$Q_I(\Delta f)^{(r)} = \frac{\sin(\Delta f/f_0\pi)}{N \sin(\Delta f/Nf_0\pi + 2\pi/N)} \sin\left(\frac{\Delta f}{f_0}\pi\left(1 + \frac{1}{N} - \frac{2}{N}r\right) + \frac{2\pi}{N}\right) \quad (22)$$

The exact (compensated) voltage and current phasors, as calculated by Equation (18), are down sampled at four samples per cycle in order to provide signals that are synchronous with the 240 Hz thread where the protection algorithms operate. In Figure 3, a schematic diagram of the real-time data-acquisition and phasor extraction SIMULINK modules is shown.

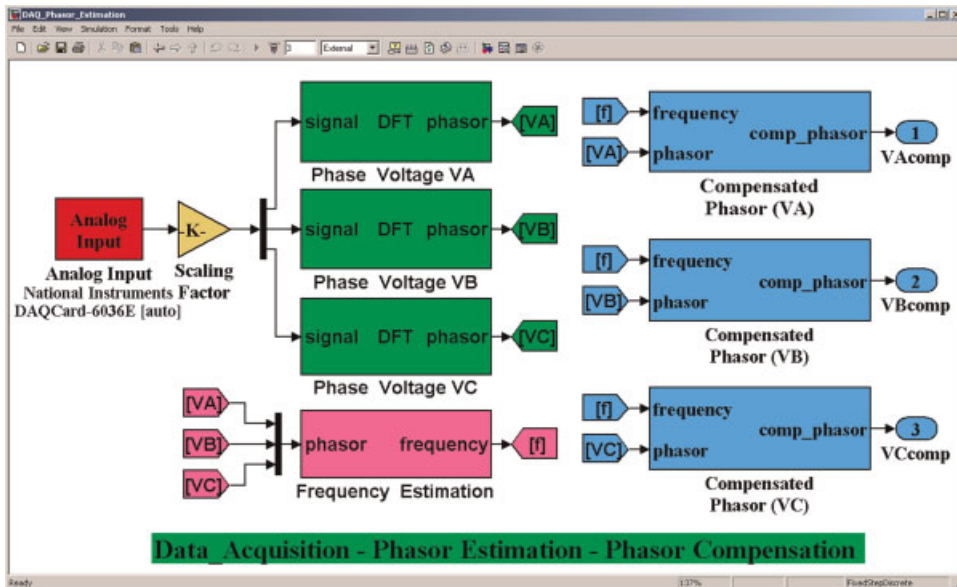


Figure 3. Real-time acquisition and phasor extraction modules.

Table II. Main protection functions of the digital relay model.

Protection functions
Phase distance element (2 zones)
Ground distance element (2 zones)
Phase time overcurrent element
Ground time overcurrent element

3.3. Protection functions

The main protection functions of the digital relay model are shown in Table II.

3.3.1. Phase and ground distance elements. The phase and ground distance protection elements utilize six Mho comparator units, with positive sequence memory polarization, to detect six of the seven possible types of faults encountered in a power system [16], as listed in Table III. The three phase-to-phase fault elements also detect the seventh fault type, which is a three phase-to-ground fault.

The Mho comparator unit comprises an operating quantity, $\overline{S1} = m\overline{Z_L} \times \overline{I} - \overline{U}$, and a polarizing quantity, $\overline{S2} = \overline{U_{pol}}$, which are used to calculate the generated torque as follows:

$$T = \text{Re}[\overline{S1} \times \overline{S2}^*] = [(m\overline{Z_L} \times \overline{I} - \overline{U})\overline{U_{pol}}^*] \quad (23)$$

in Equation (23), T is the torque product that causes the distance element operation, if $T > 0$; m is the per-unit reach of the distance element and $\overline{Z_L}$ is the total line positive sequence impedance. Table III defines the variables \overline{U} , \overline{I} , and $\overline{U_{pol}}$ for each type of fault.

In Table III, the polarizing quantities are derived from a positive sequence voltage memory filter [17], which is given by the following formula:

$$\overline{UA1M}_k = a\overline{UA1}_k - (1 - a)\overline{UA1M}_{k-N/2} \quad (24)$$

where, $\overline{UA1}_k$ is the positive-sequence voltage, $\overline{UA1M}_k$ the memorized positive-sequence voltage at sample k , and $\overline{UA1M}_{k-N/2}$ is the half-cycle old memorized positive-sequence voltage.

The positive sequence voltage memory filter improves the fault resistance coverage of the distance elements, by expanding the Mho characteristic all the way back to the source impedance, and provides reliable fault detection for zero voltage three-phase faults. The parameter a in Equation (24) defines the memory time constant or the length of the polarizing memory and has been set equal to 1/32 [18].

Finally, the phase and ground distance elements calculate the impedance of the line involved in each fault type, by solving Equation (23) for m (the per-unit reach) as follows:

$$|Z| = m|\overline{Z_L}| = \frac{\text{Re}(\overline{U} \times \overline{U_{pol}}^*)}{\text{Re}(\overline{Z_L}/|\overline{Z_L}|\overline{I} \times \overline{U_{pol}}^*)} \quad (25)$$

Table III. Voltages and currents for six Mho comparator units.

Fault type	Voltage \overline{U}	Current \overline{I}	Polarization $\overline{U_{pol}}$	Torque T
A-G	\overline{UA}	$\overline{IA} + k\overline{0} \times \overline{IG}$	$\overline{UA1mem}$	T_{ag}
B-G	\overline{UB}	$\overline{IB} + k\overline{0} \times \overline{IG}$	$\overline{UB1mem}$	T_{bg}
C-G	\overline{UC}	$\overline{IC} + k\overline{0} \times \overline{IG}$	$\overline{UC1mem}$	T_{cg}
A-B	$\overline{UA} - \overline{UB}$	$\overline{IA} - \overline{IB}$	$-j\overline{UC1mem}$	T_{ab}
B-C	$\overline{UB} - \overline{UC}$	$\overline{IB} - \overline{IC}$	$-j\overline{UA1mem}$	T_{bc}
C-A	$\overline{UC} - \overline{UA}$	$\overline{IC} - \overline{IA}$	$-j\overline{UB1mem}$	T_{ca}
		$k\overline{0} = \frac{(\overline{Z_{0L}}/\overline{Z_{1L}}-1)}{3}$	$\overline{IG} = \overline{IA} + \overline{IB} + \overline{IC}$	

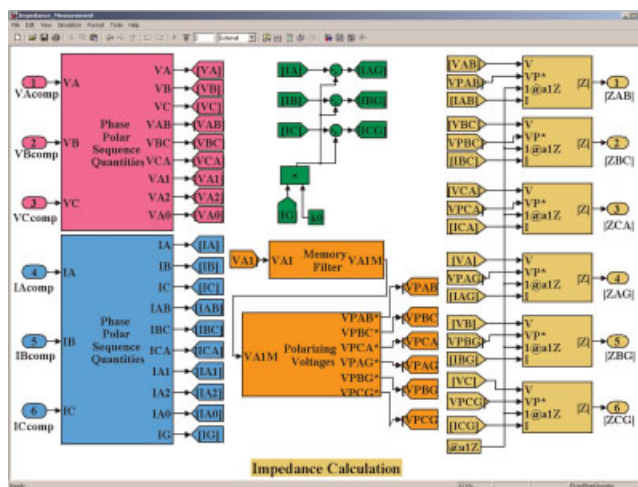


Figure 4. Impedance calculation module.

This computed impedance is compared to the user-defined settings for each zone of the distance relay to obtain a trip operation. An illustration of the distance protection elements, being developed in SIMULINK environment, is shown in Figure 4.

3.3.2. *Phase and ground overcurrent elements.* The phase and ground time overcurrent elements have been developed using the algorithm [19,20] shown in Figure 5:

In Figure 5, I is the maximum phase current magnitude, $M = I/I_{pu}$ the multiple of the pickup current setting I_{pu} , TD the time dial setting, t_m the curve operating time for $M > 1$, t_r is the reset time delay for $M \leq 1$, Δt the processing time of the protection function, and A, B, P are constants that define the inverse-time relay operating characteristic.

Figure 6 illustrates the phase time O/C element created in SIMULINK along with its editing mask.

4. EXAMPLE CASES

A sample power system model has been created using the RSCAD software (Figure 7) which includes the following components:

- two equivalent source models,
- a faulted transmission line model,
- circuit breaker models,
- current transformer (CT) models monitoring the three phase current at the relay point,
- voltage transformer (VT) models monitoring the phase-to-neutral voltages at the relay point,
- control switches defining the characteristics of the applied faults: fault type, fault location, fault duration, fault angle, etc.

The digital relay model developed in SIMULINK is integrated with the real-time power system model in the RTDS as described in Section 2.3. Several operating and fault conditions have been simulated in order to validate the digital relay model. Following, two example cases are provided for demonstrating the real-time implementation and validation of the digital relay model using the proposed integrated environment. The parameters of the power system model and the settings of the digital relay model used are given in the Appendix.

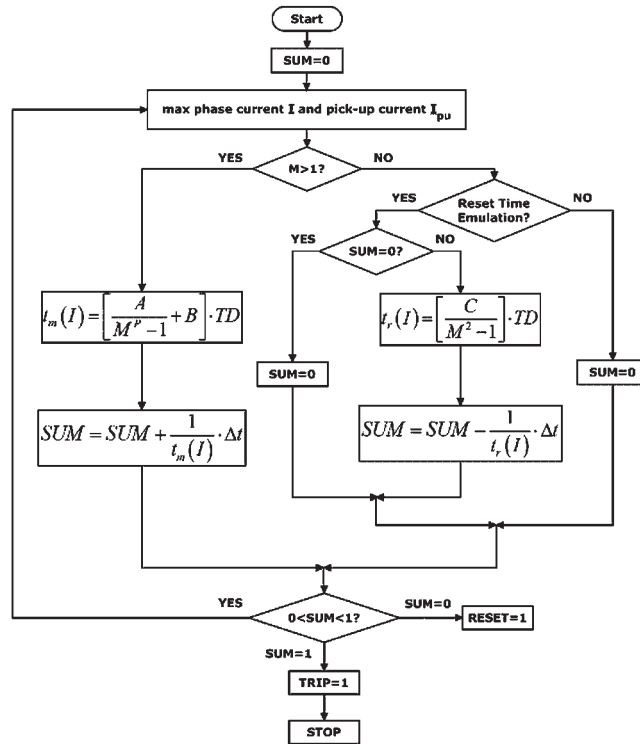


Figure 5. Flow chart for the overcurrent relay element operation.

4.1. Example case 1

Figure 8 shows the results of a real-time simulation test for a single line-to-ground fault involving phase B at 75% length of the transmission line. Figure 9 shows the instantaneous secondary voltage and current at phase B acquired from the digital relay model for the same test case.

Due to the fact that the real-time simulation of the power system model in the RTDS and the real-time execution of the digital relay model run in parallel without time synchronization, there is a very short time-delay in the displays obtained from the RTDS and the ones obtained from the digital relay model. This, however, does not affect the interaction of the two systems.

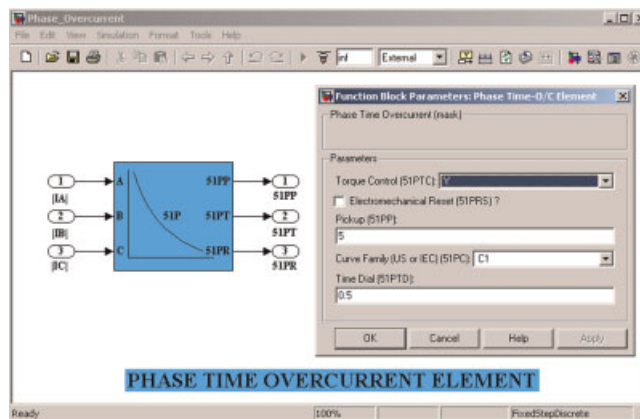


Figure 6. Phase time overcurrent element.

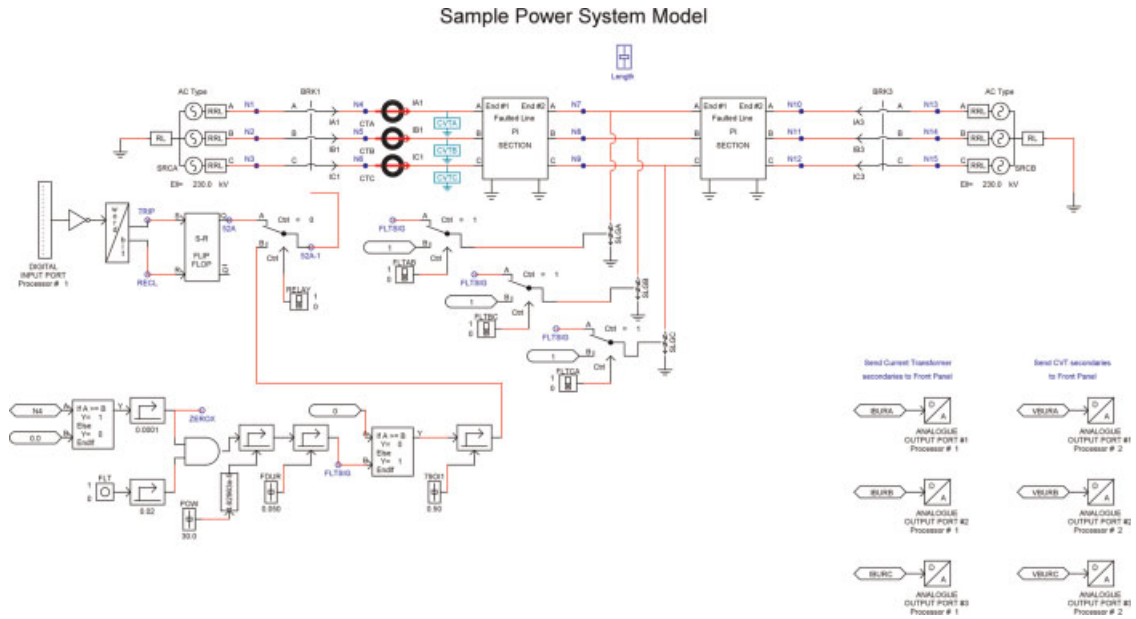


Figure 7. Sample power system model as simulated in the RTDS.

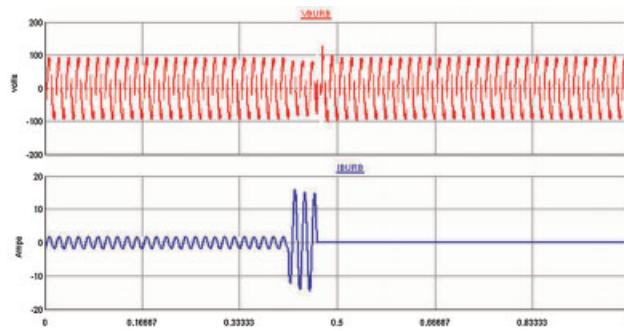


Figure 8. B-G fault at 75% of the line—instantaneous secondary voltage and current at phase B simulated in the RTDS.

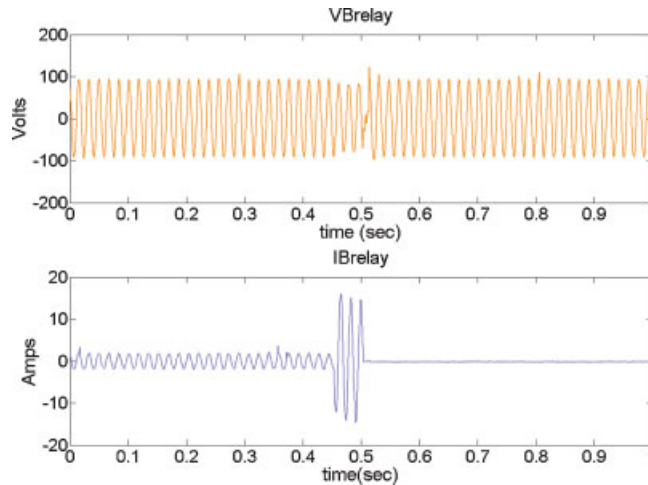


Figure 9. B-G fault at 75% of the line—instantaneous secondary voltage and current at phase B acquired from the digital relay model.

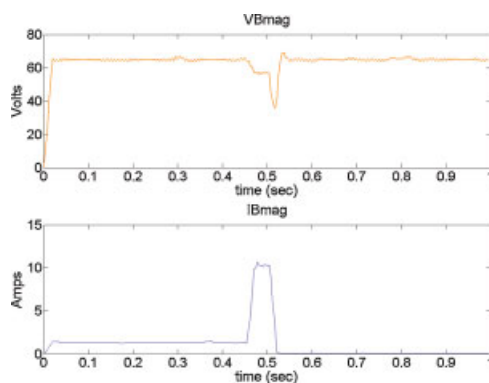


Figure 10. B-G fault at 75% of the line—instantaneous secondary voltage and current rms magnitudes at phase B acquired from the digital relay model.

The digital relay model reproduces correctly the signals received from the RTDS, as can be seen in Figure 9. Furthermore, it estimates the rms magnitudes of the faulted phase voltage and current (Figure 10). Finally, it detects the fault in the first zone of the distance ground element and issues a non-delayed trip command (Figure 11). The trip command is assigned to a digital output port of the DAQ system which controls the status of the associate circuit breaker in the RTDS simulation. This circuit breaker has been given an open delay time equal to one cycle. When the trip command is equal to logical “1,” it opens the circuit breaker which clears the fault from the relay side (Figures 8–10).

4.2. Example case 2

A phase-to-phase fault between phases A and B has been simulated at 70% length of the transmission line, in order to check the response of the time overcurrent phase element. Figures 12 and 13 show the instantaneous secondary currents of the faulted phases captured from the RTDS and the digital relay model, respectively.

Figure 14 illustrates the current rms magnitudes of the faulted phases A and B, which are used as inputs to the time overcurrent phase element.

The time overcurrent phase element provides two logical output signals that define its state: the 51P signal becomes logical “1” when the maximum of the phase current rms magnitude exceeds the pickup current setting of the element; the 51PT signal becomes logical “1” when the accumulated time of the emulated relay travel disk exceeds the time dial setting.

These logical signals are shown in Figure 15 for the fault case studied. By subtracting the rising edge times of the two signals, the operating time of the time overcurrent phase element is calculated, which is equal to $t_{m_calc} = t_2 - t_1 = 0.2375$ second.

The time overcurrent phase element settings selected are shown in the Appendix. By using these settings and the average of the maximum current rms magnitudes obtained from the digital relay model shown in Figure 14, one may calculate the expected

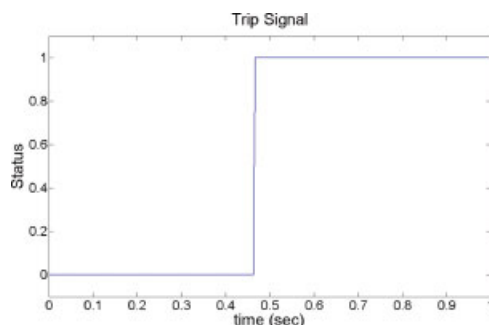


Figure 11. B-G fault at 75% of the line—trip command issued from the digital relay model.

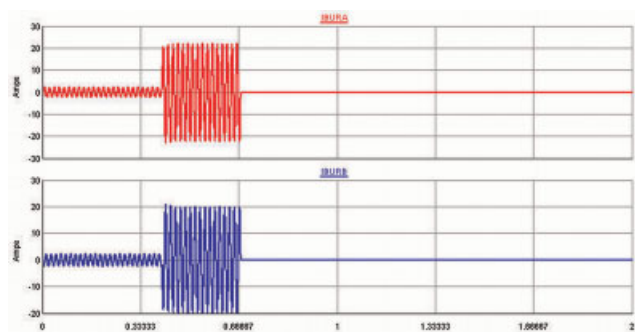


Figure 12. A-B Fault at 70% of the line—instantaneous secondary currents at phase A and B simulated in the RTDS.

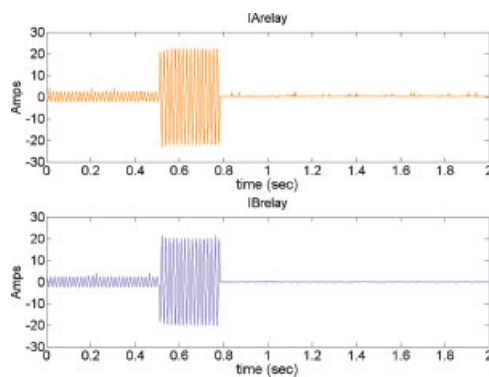


Figure 13. A-B fault at 70% of the line—instantaneous secondary currents at phase A and B acquired from the digital relay model.

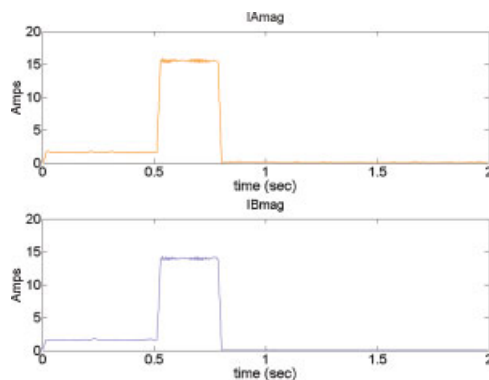


Figure 14. A-B fault at 70% of the line—instantaneous secondary current rms magnitudes at phase A and B acquired from the digital relay model.

operating time for the time overcurrent phase element. This is equal to $t_{m_exp} = 0.2372$ second, using the data available in the Appendix and considering $I = 15.6$ A (Figure 14).

It can be seen that there is only a slight difference between the operating time calculated from the digital relay model and the expected time derived from the characteristic curve for the given current I . This is an indication of the adequate design of the time overcurrent phase element.

After 51PT becomes “high,” the fault is cleared by opening the associate circuit breaker in the RTDS simulation after 0.02 second, which is the circuit breaker opening time (Figures 12–14).

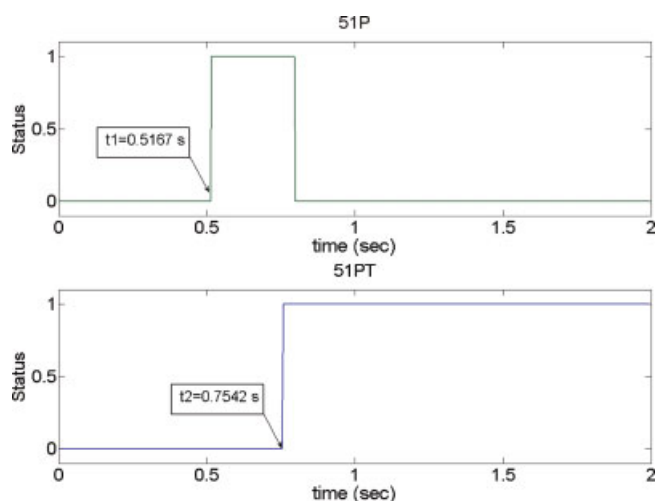


Figure 15. A-B fault at 70% of the line—51P and 51PT logical signals issued from the digital relay model.

5. CONCLUSIONS

This paper has demonstrated an integrated environment based on MATLAB/SIMULINK and RTDS for real-time implementation and validation of digital relay models. The paper has provided an overview of the proposed environment, as well as its hardware and software requirements. Modeling issues associated with digital relays are also discussed.

Although a certain “setup” of the protective relay (algorithms, filtering, sampling rate, etc.) has been studied, it is evident that the proposed platform can be a very effective tool for the development of new protective devices and the analysis of the existing ones.

The example study cases given focus mainly on distance and overcurrent protection relay elements. Nevertheless, sufficient details are provided for the general capabilities and features of the proposed environment.

6. LIST OF SYMBOLS AND ABBREVIATIONS

\bar{D}	frequency deviation phasor
\bar{D}'	filtered-frequency deviation phasor
$\bar{D}'^{(r)}$	filtered-frequency deviation phasor at time sample r
$\bar{D}_{a,b,c}$	phase deviation phasors
$\bar{D}_{a,b,c}^{(r)}$	phase deviation phasors at time sample r
f	actual system frequency
f_0	fundamental system frequency
$f^{(r)}$	actual system frequency at time sample r
m	per unit reach of the distance element
N	number of samples per cycle
ΔT	time interval between samples
t_c	time constant of 1st order digital low-pass
$\bar{U}_{a,b,c}$	phase voltage phasors
$\bar{U}_{a,b,c}^{(r)}$	phase voltage phasors at time sample r
$\bar{U}_{a,b,c}^{(r)*}$	complex conjugate of phase voltage phasors at time sample $r - 1$
$U_{a,b,c} \text{Re}^{(r)}$	real part of phase voltage phasors at time sample r
$U_{a,b,c} \text{Re}^{(r-1)}$	real part of phase voltage phasors at time sample $r - 1$
$U_{a,b,c} \text{Im}^{(r)}$	imaginary part of phase voltage phasors at time sample r

$U_{a,b,c1}^{(r-1)}$	imaginary part of phase voltage phasors at time sample $r - 1$
$\overline{UA1}_k$	positive-sequence voltage at time sample k
\overline{UAIM}_k	positive-sequence memory voltage at time sample k
$\overline{X}^{(r)}$	complex phasor of the measured signal $x(t)$ at time sample r
$x(k\Delta T)$	sampled-discrete value of the measured signal $x(t)$
$X_R^{(r)}$	real part of the phasor \overline{X} at time sample r
$X_I^{(r)}$	imaginary part of the phasor \overline{X} at time sample r
\overline{Z}_L	total line positive sequence impedance

REFERENCES

1. McLaren PG, Henville C, Skendzic V, *et al.* Software models for relays. *IEEE Transactions on Power Delivery* 2001; **16**(2):238–246.
2. Luo X, Kezunovic M. Interactive protection system simulation using ATP models and C++. *IEEE PES 2005 Transmission & Distribution Conference & Exposition*, Dallas, Texas, May 2006.
3. Kezunovic M, Kasztenny B. New SIMULINK libraries for modeling digital protective relays and evaluating their performance under fault transients. *Proceedings of ICDS '97*, Montreal, Quebec, 28–30 May 1997.
4. McLaren PG, Dirks EN, Jayasinghe RP, *et al.* An accurate software model of a digital relay for use in off-line studies. *IEEE Transactions on Power Delivery* 1995; **10**(2):666–675.
5. Dysko A, McDonald JR, Burt GM, *et al.* Integrated modeling environment: a platform for dynamic protection modeling and advanced functionality. *IEEE PES Transmission & Distribution Conference*, April 1999.
6. Wu J, Cheng Y, Srivastava AK, *et al.* Hardware in the loop test for power system modeling and simulation. *IEEE PES Power Systems Conference & Exposition, PSCE*, 29 October - 1 November 2006.
7. Kuffel R, Giesbrecht J, Maguire T, *et al.* RTDS—a fully digital power system simulator operating in real time. *Proceedings of ICDS-95*, College Station, USA, April 1995.
8. McLaren PG, Kuffel R, Wierckx R, *et al.* A real time digital simulator for testing relays. *IEEE Transactions on Power Systems* 1992; **7**(1):207–213.
9. Kezunovic M, Kasztenny B, Galijasevic Z. Modeling, developing and testing protective relays using MATLAB, programmable relays and digital simulators. *Third International Conference on Digital Power System Simulators-ICDS'99*, Vasteras, Sweden, May 1999.
10. *Matlab User's Guide*. Real-time Workshop, Version 6.3, The MathWorks Inc., 2005.
11. *Matlab User's Guide*. Real-time Windows Target, Version 2.6, The MathWorks, 2005.
12. Premerlani WJ. Means and methods for measuring power system frequency, US Patent 4547726, 15 October 1985.
13. Sidhu TS. Accurate measurement of power system frequency using a digital signal processing technique. *IEEE Transactions on Instrumentation and Measurement* 1999; **48**(1):75–81.
14. Premerlani WJ. Method and apparatus for compensation of phasor estimations, US Patent 6141196, 31 October 2000.
15. Benmoulay G. System and method for exact compensation of fundamental phasors, US Patent 6934654, 23 August 2005.
16. Roberts J, Guzman A, Schweitzer EO-III, *et al.* $Z = V/I$ does not make a distance relay. *20th Annual Western Protective Relay Conference*, Spokane, Washington, 19–23 October 1993.
17. Schweitzer EO. III New developments in distance relay polarization and fault type selection. *16th Annual Western Protective Relay Conference*, Spokane, WA, October 1989.
18. Hou D, Guzman A, Roberts J. Innovative solutions improve transmission line protection. *24th Annual Western Protective Relay Conference*, Spokane, WA, 21–23 October 1997.
19. Mooney JB, Hou D, Henville CF, Plumtre FP. Computer-based relay models simplify relay application studies. *20th Western Protective Relaying Conference*, Spokane, Washington, 19–21 October 1993.
20. Tan JC, McLaren PG, Jayasinghe RP, Wilson PL. Software model for inverse time overcurrent relays incorporating IEC and IEEE standard curves. *CCECE '02, Canadian Conference on Electrical and Computer Engineering*, 2002.

APPENDIX

Sample power system model data

- (1) Power frequency: 60 Hz
- (2) Equivalent source at the left terminal of the transmission line:

$$E_A = 230 \angle 0^\circ \text{ kV}, Z_{A0} = 12,8 \angle 73.6^\circ \Omega, Z_{A+} = 3,77 \angle 81.2^\circ \Omega$$

- (3) Equivalent source at the right terminal of the transmission line:

$$E_B = 230 \angle 0^\circ \text{ kV}, Z_{B0} = 12.8 \angle 73.6^\circ \Omega, Z_{B+} = 3.77 \angle 81.2^\circ \Omega$$

- (4) Transmission line data: ($R_{L+} = 0.018547 \Omega/\text{km}$, $L_{L+} = 0.99898 \times 10^{-3} \text{ H/km}$, $C_{L+} = 11.64 \times 10^{-9} \text{ F/km}$)
 ($R_{L0} = 0.3618376 \Omega/\text{km}$, $L_{L0} = 3.2567 \times 10^{-3} \text{ H/km}$, $C_{L0} = 7.686 \times 10^{-9} \text{ F/km}$).
- (5) Transmission line length: 100 km,
- (6) CT ratio: 1200/5 A,
- (7) VT ratio: 230 kV/115 V.

DIGITAL RELAY MODEL SETTINGS

Elements		Setting (% length of Z_{L+})	Time delay setting (second)
Phase distance	Zone1	80	0.00
	Zone2	150	0.30
Ground distance	Zone1	80	0.00
	Zone2	150	0.30

Elements	Pickup current (secondary)	Time dial setting	Curve selection
Phase TOC	5A	0.5	U1
Ground TOC	1A	0.5	U1

Time-overcurrent curves US moderately inverse curve: U1

$$t_m = \text{TD} \left(0.0226 + \frac{0.0104}{M^{0.02} - 1} \right)$$

$$t_r = \text{TD} \left(\frac{0.0104}{1 - M^2} \right)$$